Figure S1

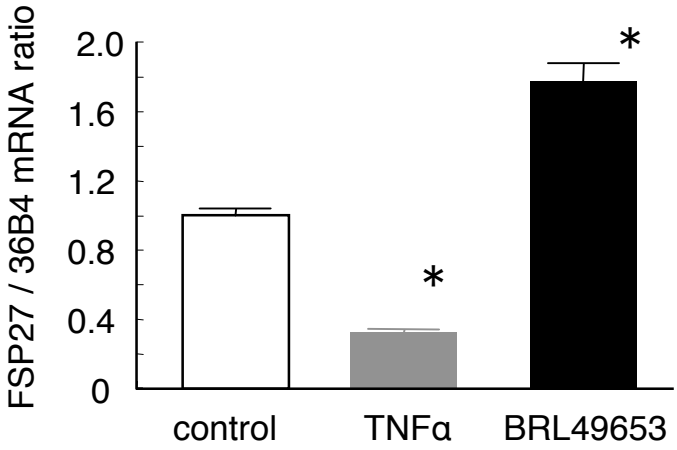

Figure S2

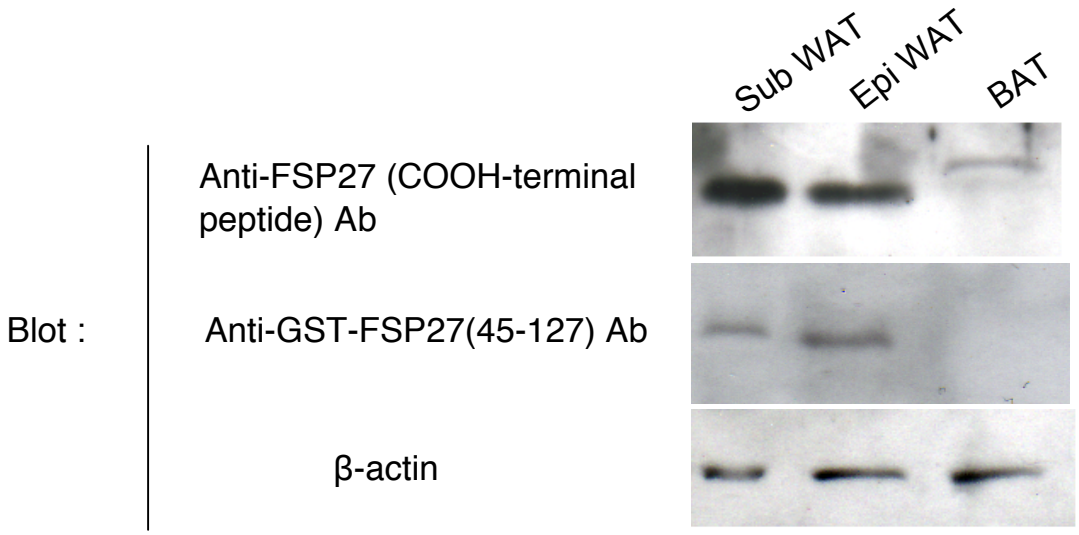

Figure S3

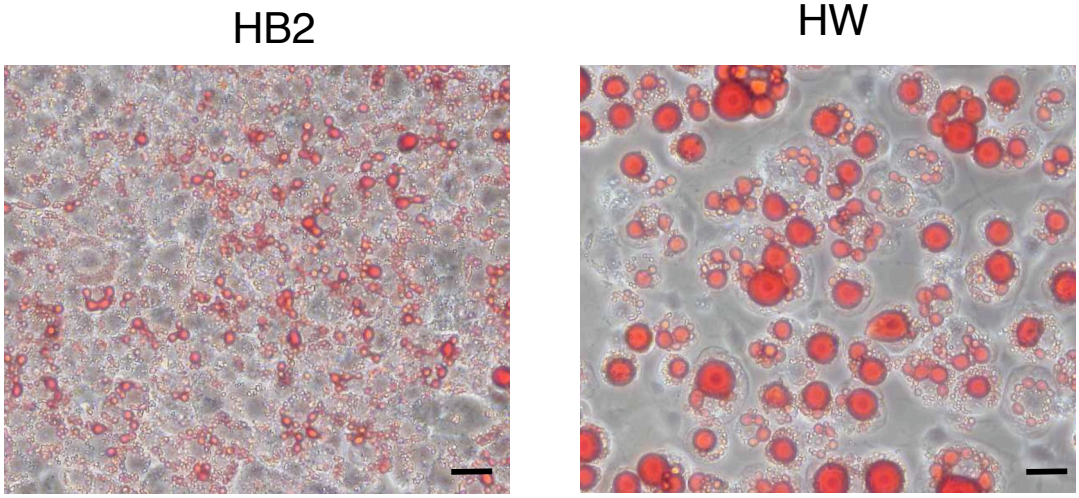

Figure S4

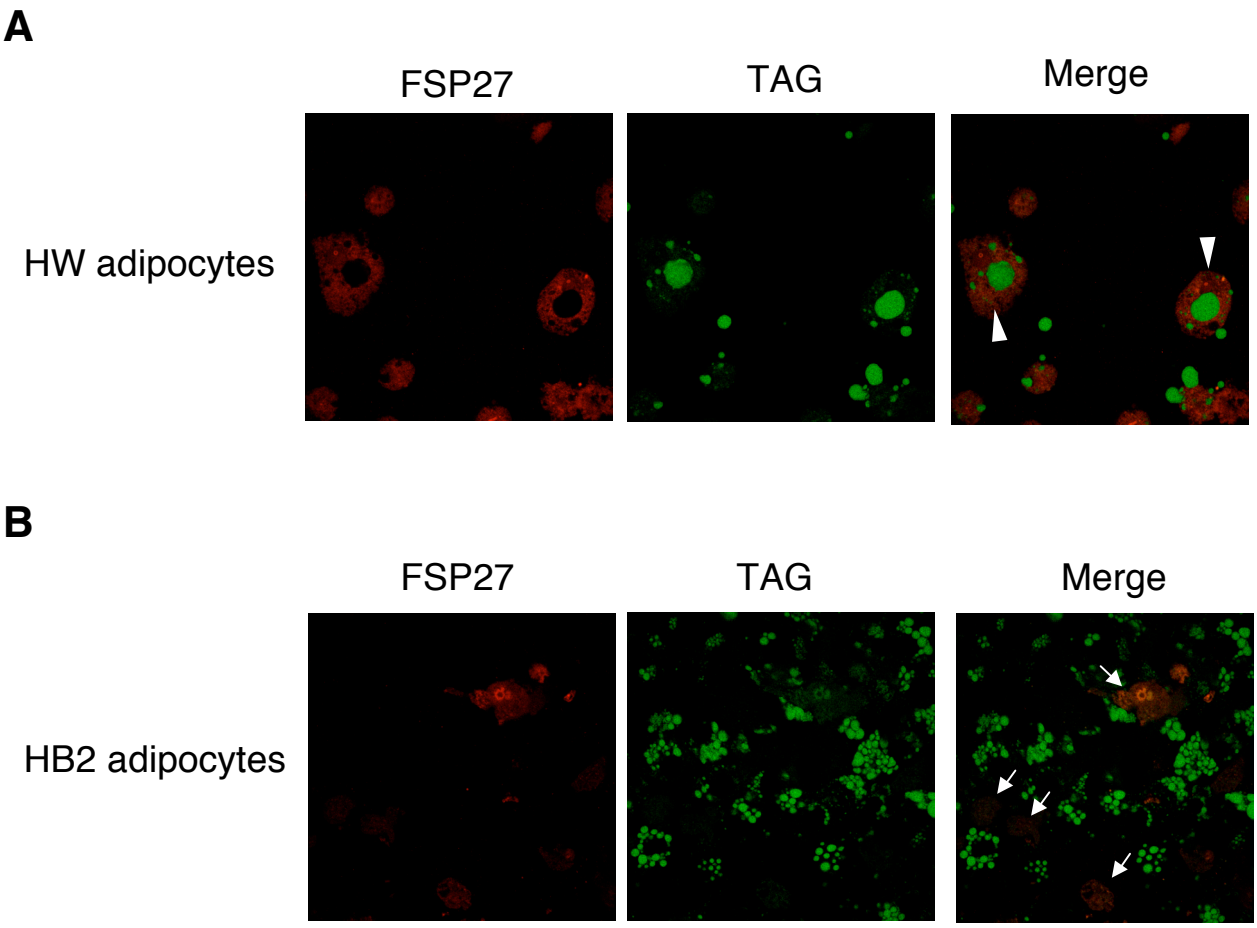
A
FSP27
TAG
Merge
HW adipocytes
B
FSP27
TAG
Merge
HB2 adipocytes

Figure S5

A

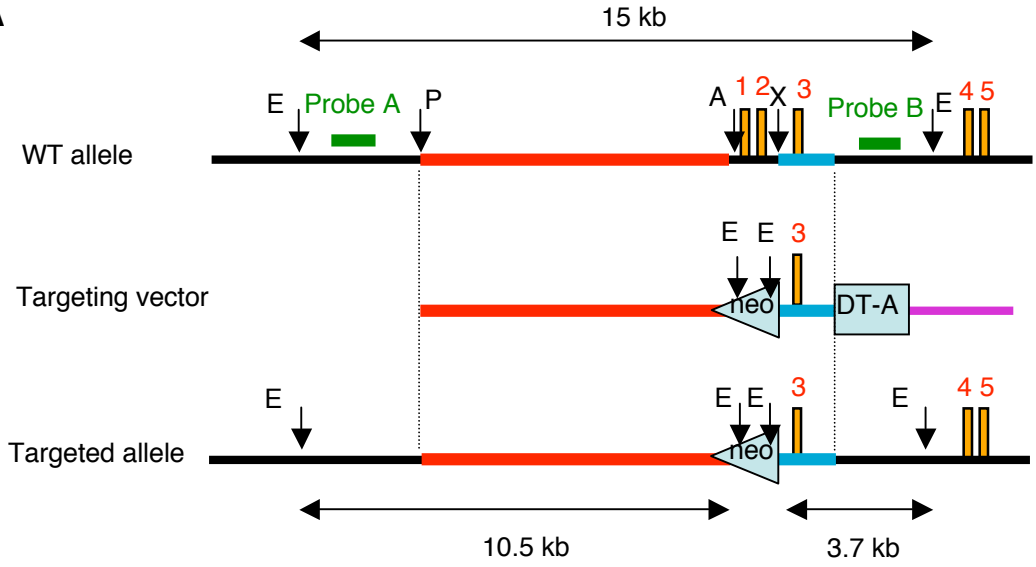

B

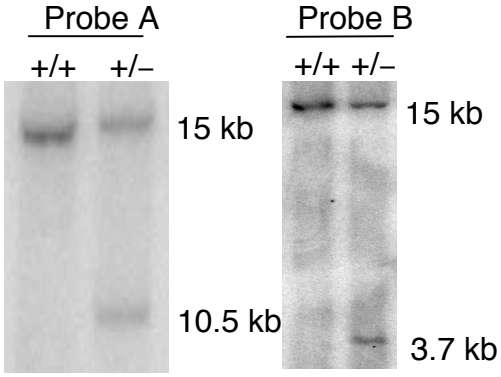

C

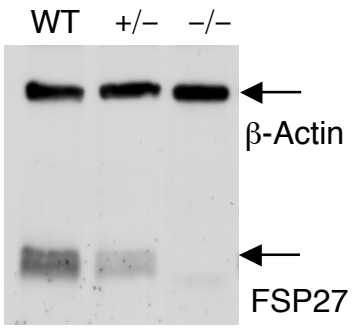

Figure S6

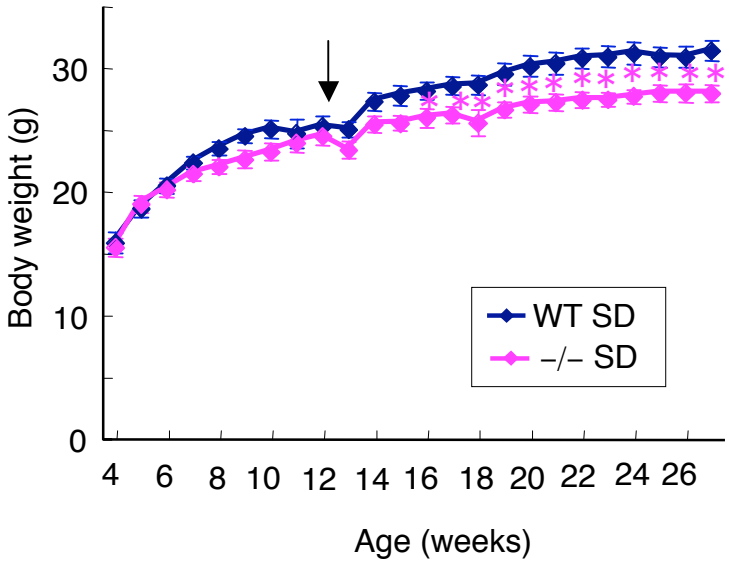

Figure S7

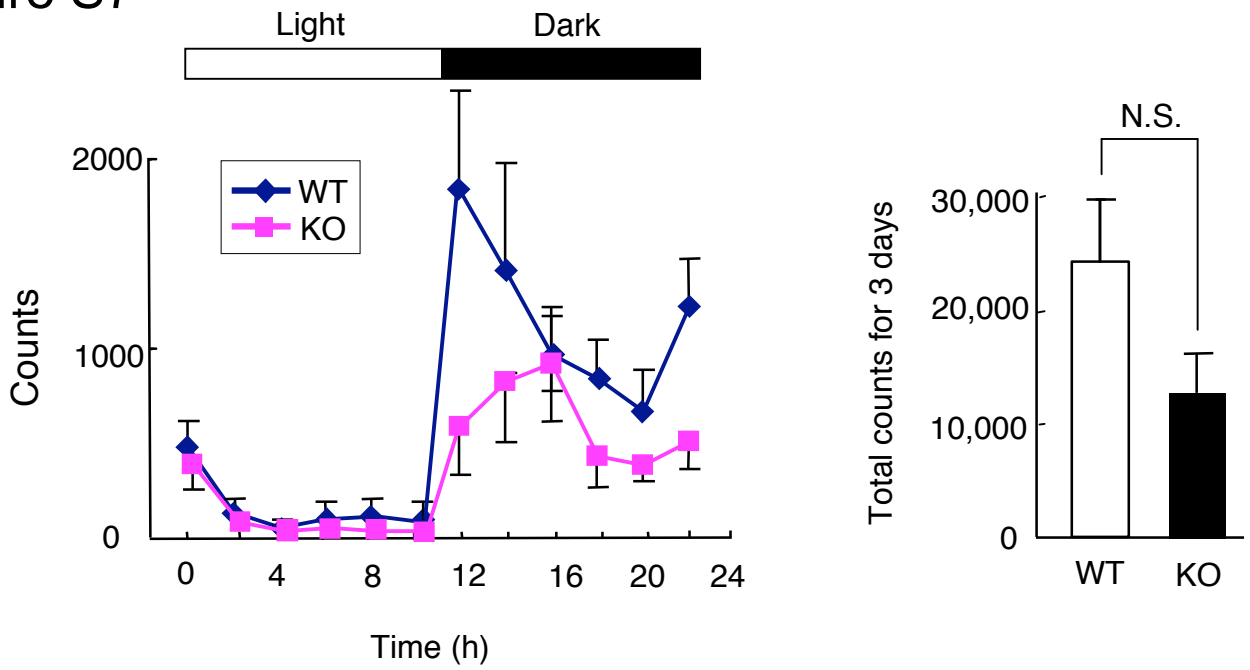

Figure S8

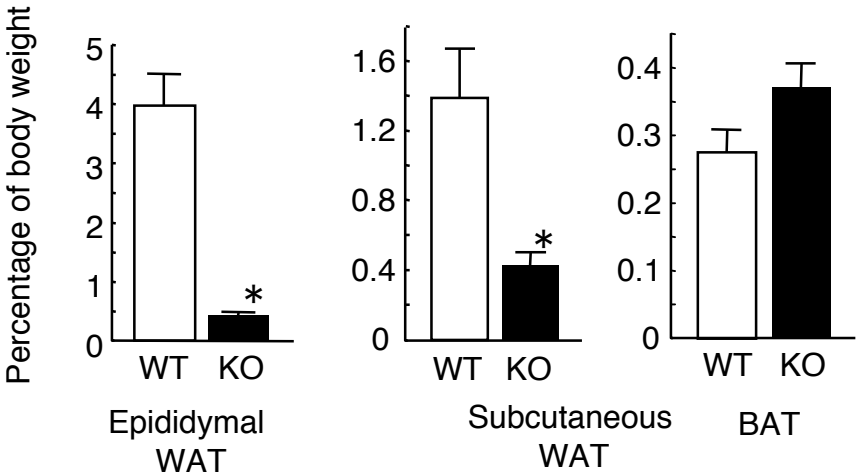

Figure S9

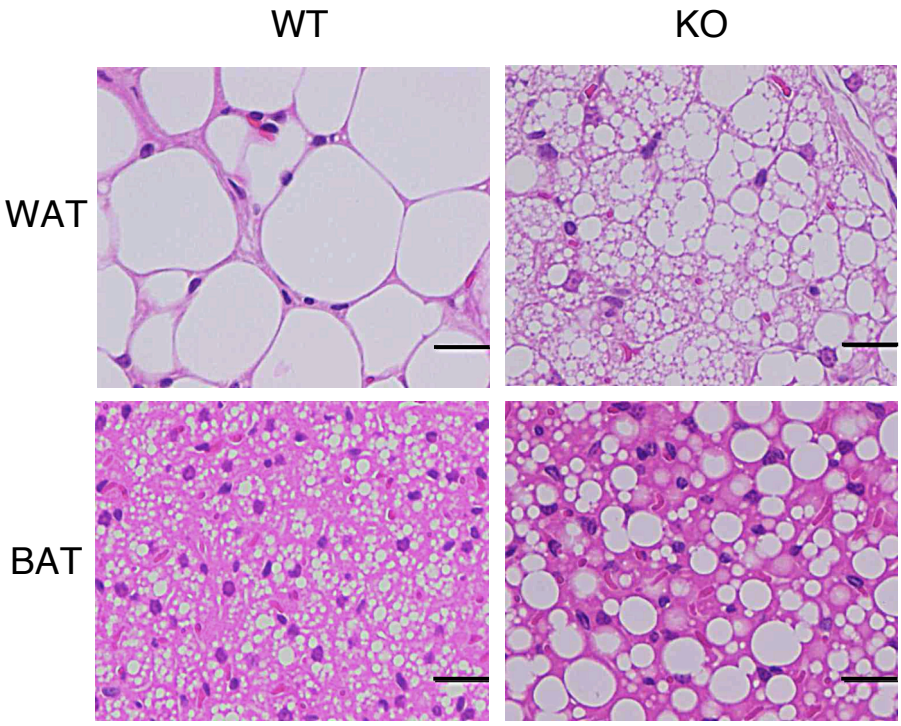

Figure S10

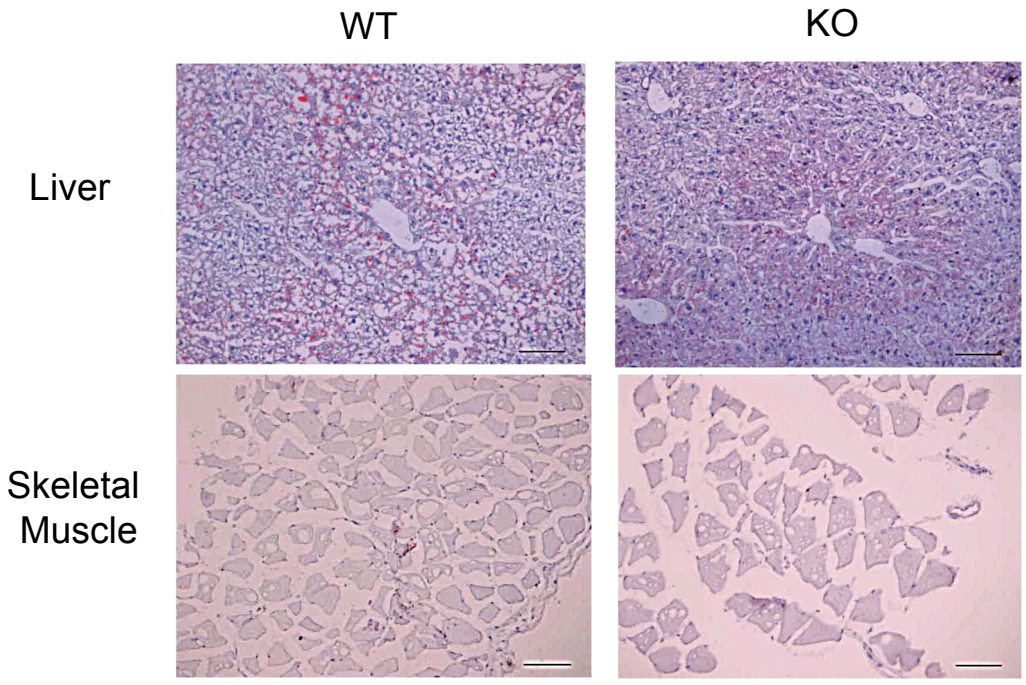

Figure S11

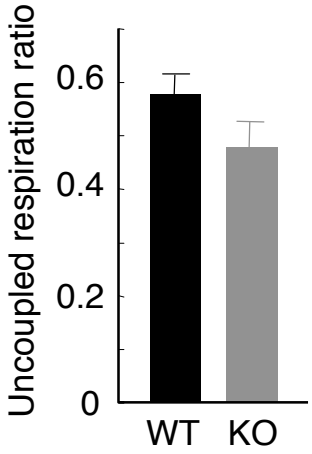

Figure S12

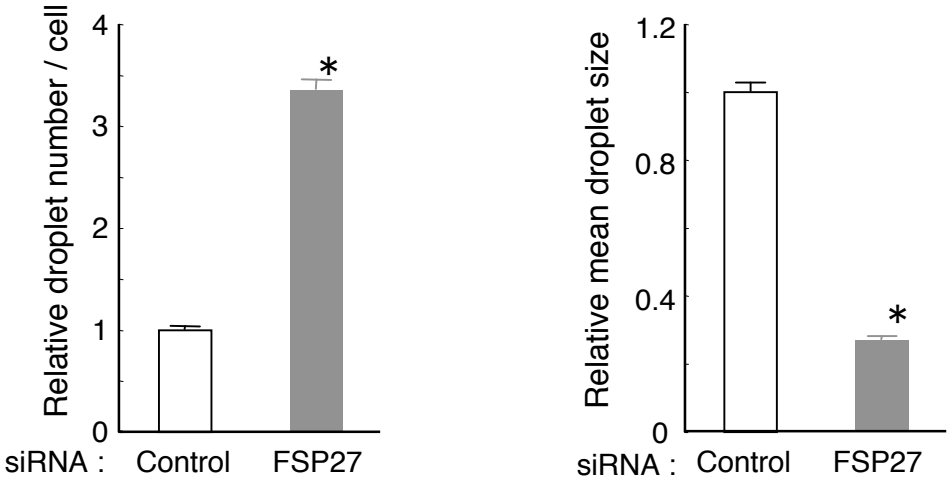

Figure S13

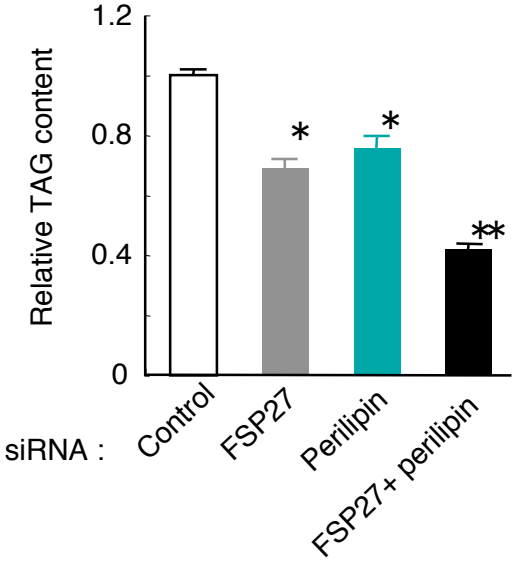

Supplemental Data

Figure S1. Quantitative RT-PCR analysis of FSP27 mRNA in 3T3-L1 adipocytes incubated for 48 h in the absence (control) or presence of TNF-α (10 ng/ml) or 5 μM BRL49653. Data were normalized by the amount of 36B4 mRNA and expressed relative to the corresponding value for control cells; they are means ± SEM from three independent experiments. *$P < 0.01$ versus control.

Figure S2. Immunoblot analysis of FSP27 in total lysates of isolated adipocytes from subcutaneous (Sub) WAT, epididymal (Epi) WAT, and BAT of C57BL/6J mice at 18 to 19 weeks of age. The analysis was performed with antibodies generated in response to a COOH-terminal peptide of mouse FSP27 or to a GST fusion protein of mouse FSP27 (amino acid residues 45 to 127).

Figure S3. Lipid accumulation in HB2 and HW adipocytes. Neutral lipid was stained with oil red O at 7 days after the onset of induction of adipogenesis. Scale bars, 20 μm.

Figure S4. Immunofluorescence localization of ectopic FSP27 in HW white (**A**) and HB2 brown (**B**) adipocytes. The cells were infected with an adenovirus encoding mouse FSP27 tagged at its COOH-terminus with the Flag epitope. They were then subjected to immunofluorescence analysis with antibodies to the Flag tag as well as to staining of TAG with Bodipy 493/503. Merged images are also shown. Arrowheads and arrows indicate mature HW adipocytes and HB2 preadipocytes, respectively.

Figure S5. Generation of FSP27 knockout mice. **A**, Schematic representation of the wild-type (WT) *Fsp27* allele, the targeting vector, and the targeted allele after homologous recombination. Exons are indicated by yellow boxes. Probes A and B are DNA fragments used for Southern blot analysis of Eco RV–digested genomic DNA from embryonic stem cells. neo, neomycin resistance gene; DT-A, gene for the A chain of diphtheria toxin; E, Eco RV; P, Pst I; A, Apa I; X, Xho I. **B**, Southern blot analysis of Eco RV–digested DNA from embryonic stem cells. The wild-type and mutant *Fsp27* alleles give rise to 15- or 10.5-kb (probe A) or 15- or 3.7-kb (probe B)

hybridizing fragments, respectively. *Fsp27* genotype is indicated above each lane. **C**, Immunoblot analysis of total extracts of WAT from wild-type (WT), FSP27 heterozygous knockout (+/–), and FSP27 homozygous knockout (–/–) mice with antibodies to FSP27 and to β-actin (control).

Figure S6. Body weight of wild-type (WT) and FSP27 homozygous knockout (–/–) mice maintained on a standard diet (SD) from 4 to 27 weeks of age. Data are means ± SEM [n = 12 (WT) and 9 (–/–)]. *P < 0.05 versus corresponding value for wild-type mice. Arrow shows the fasting of mice for metabolic analysis.

Figure S7. Locomotor activity in FSP27-KO mice. Locomotor activity during a 12-h-light, 12-h-dark cycle (left panel) and total locomotor activity during three consecutive cycles (right panel) for 12-week-old mice. Data are means ± SEM [n = 3 for wild type (WT), n = 4 for FSP27-KO (KO)]. N.S., not significant.

Figure S8. Weights of epididymal WAT, subcutaneous WAT, and BAT isolated from 14-week-old wild-type (WT) and FSP27-KO (KO) mice maintained on a high-fat diet for 10 weeks. Data are means ± SEM (n = 4 to 8). *P < 0.01 versus corresponding value for wild-type.

Figure S9. Sections of subcutaneous WAT and interscapular BAT from 14-week-old wild-type (WT) and FSP27-KO (KO) mice were stained with hematoxylin-eosin and examined by light microscopy. Scale bars, 20 μm.

Figure S10. Oil red O staining of sections of liver and skeletal muscle from 45-week-old male wild-type (WT) and FSP27-KO (KO) mice. Scale bars, 100 μm.

Figure S11. Uncoupled respiration ratio for adipocytes isolated from inguinal WAT of wild-type (WT) and FSP27-KO (KO) mice at 16 to 20 weeks of age. Data are expressed as the ratio of oxygen consumption not devoted to ATP synthesis to the total oxygen consumption and are means ± SEM [n = 4 (WT) or 6 (KO)].

Figure S12. Quantitation of droplet number per cell (left panel) and mean droplet size

(right panel) after introduction of FSP27 siRNA into HW adipocytes in experiments similar to that shown in Figure 5D. Data are means ± SEM for 905 (control) or 992 (FSP27 siRNA) cells and are expressed relative to the corresponding value for control cells. *$P < 0.001$ versus control cells.

Figure S13. Intracellular TAG content of HW adipocytes 3 days after siRNA introduction as in Figure 5C. Data are means ± SEM ($n = 6$) and are expressed relative to the control value. *$P < 0.01$ versus control siRNA; **$P < 0.01$ versus FSP27 or perilipin siRNA.